

# DEVELOPMENT AND VALIDATION OF A GENERIC FLIGHT SIMULATION BASED ON AIRCRAFT GEOMETRY

K. Schreiter

TU Berlin, Institut für Luft- und Raumfahrt, Marchstr. 12, 10587 Berlin, Deutschland

## Abstract

Simulating fixed wing airplanes is a challenging field that uses different approaches to model the behavior of aircraft dynamics. In most cases flight test data for different points of the envelope are generated and used as look-up table for simulation. For existing airplanes this method is expensive and for aircraft in the preliminary design phase it is not feasible. Therefore a flight simulation has been developed, which uses solely the geometric data of the aircraft to simulate its dynamics. The first step was to design a flexible and modular structure of the complete simulation followed by the definition of appropriate module requirements. Following this specific real-time models for aerodynamics, landing gear and engine thrust have been created. The flight simulation including input/output interfaces was realized using Matlab-Simulink® and embedded C-code. A certified full flight simulator (FFS) has been used to preliminary validate the chosen approaches. The results of the validation process have proved promising with respect to this particular first step approach.

## Nomenclature

$b$	=	braking coefficient	$q$	=	pitch rate
$B$	=	brake	$r$	=	yaw rate
$C_D$	=	drag force coefficient	$S$	=	side force
$CG$	=	center of gravity	$SD$	=	spring damper
$C_L$	=	lift force coefficient	$T$	=	thrust
$C_l$	=	rolling moment coefficient	$W$	=	wing
$C_m$	=	pitching moment coefficient	$z$	=	vertical coordinate
$C_n$	=	yawing moment coefficient	$\zeta$	=	damping coefficient
$C_S$	=	side force coefficient	$\delta_a$	=	aileron deflection
$d$	=	damping constant	$\delta_e$	=	elevator deflection
$D$	=	drag	$\delta_F$	=	trailing edge flap deflection
$e$	=	Oswald factor	$\delta_r$	=	rudder deflection
$f$	=	airfoil camber	$\mu$	=	bypass ratio
$F$	=	force	$\mu_g$	=	glide friction coefficient
$g$	=	acceleration due to gravitation	$\mu_r$	=	roll friction coefficient
$H$	=	horizontal stabilizer	$\alpha$	=	angle of attack
$k$	=	spring stiffness	$\beta$	=	angle of sideslip
$L$	=	lift	$\Delta$	=	deviation
$l$	=	wing chord	$\varepsilon$	=	generic angle
$LG$	=	landing gear	$\eta_T$	=	thrust effectiveness factor
$m$	=	mass	$\Theta$	=	pitch angle
$Ma$	=	Mach number	$\rho$	=	air density
$p$	=	roll rate, ambient pressure	$\Phi$	=	bank angle

## 1. INTRODUCTION

There are several considerations in simulating airplane flights. In addition to different aircraft systems the aircraft dynamics play a major roll. In order to simulate flight dynamics, models are needed to reproduce forces and moments of aerodynamics, thrust and landing gear. In most cases these models are based on measured aircraft data. On the one hand, this method guarantees high fidelity and since the required data are stored in look-up tables they are suited for real-time simulation. On the other hand, obtaining this information from wind tunnel measurements or flight test campaigns is very expensive. However, this is the most accurate method for flight simulations intended for pilot training with existing types of aircraft. Nevertheless, for non-existing aircraft this method is not feasible.

For research or development, initial tests of flight

dynamical behavior are necessary to validate the design. The primary information available when an aircraft is designed is its shape which is characterized by geometry. The geometric data alone enable a modeling of the principal flight dynamics using for example finite element methods to solve the aerodynamic problem. These solutions are able to accurately describe the flight dynamics, but most of the methods require extensive time and computing capacity.

This paper is a summary of the author's diploma thesis [1] and offers a solution for simulating a fixed wing aircraft in real-time using geometric information only and is organized as follows: It starts with an overview of a complete modular flight simulation and the classification of flight dynamics. Next follows a description of modeling the geometry based simulation of flight dynamics, and finally a preliminary validation of the solution with a certified full flight simulator (FFS) will be presented.

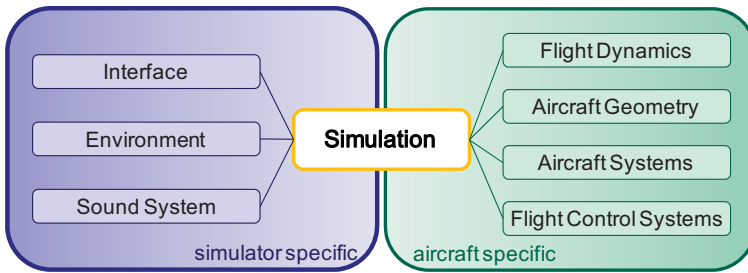


Figure 1: Framework Structure of the Simulation

	$\alpha$	$\beta$	$p$	$q$	$r$	$\delta_e$	$i_H$	$\delta_s$	$\delta_a$	$\delta_r$
$C_D$	X			X		X	X	X	X	
$C_S$		X	X		X					X
$C_L$	X			X		X	X	X	X	
$C_l$		X	X		X				X	X
$C_m$	X			X		X	X	X	X	
$C_n$		X	X		X				X	X

Table 1: Correlations considered between state variables, control surface deflections and aerodynamic coefficients

## 2. SIMULATION MODULES AND SPECIFICATIONS

The work presented here will provide the basis of a complete simulation system. Thus it is necessary to specify the structure of the simulation and the requirements it has to fulfill. A modular implementation of the functions facilitates the maintenance, flexibility of having exchangeable modules, and different degrees of simulation accuracy. However, a definition of interfaces is required before the modules are built. Therefore the suggested simulation framework and its requirements are set in this section.

### 2.1. Framework Structure

The first level of structuring divides simulation elements specific to the aircraft itself and the simulator specific functions (see Figure 1). The latter are the Interface between pilot and simulation, the simulation of the Environment and the Sound System. These are independent of aircraft type. The aircraft dependent modules are classified into Flight Dynamics, Aircraft Geometry, Aircraft Systems and Flight Control Systems.

In the Flight Dynamics module the behavior of the aircraft is simulated and is subdivided into Mass & CG, Aerodynamics, Equations of Motion and System Update. The Aircraft Systems module includes further subdivisions for Actuators, Landing Gear, Engines, Hydraulics, Fuel System, Navigation and Emergency. Aircraft Systems module is mainly used for display purposes. Additionally Landing Gear and Engines produce forces and moments that are also needed to simulate the flight dynamics. The Flight Control Systems module includes all units impacting Aircraft Systems, such as Auto Flight System, Flight Control System and Engine Control System.

In this paper the main focus is the Aircraft Geometry module, which represents the user interface for the simulation, and Flight Dynamics module. For any single part of the total simulation interfaces to other modules have to be specified. Every interface contains a description that includes which part is connected and what parameters are drawn. This specification assures that in and out-puts of every module are compatible and all the required parameters are calculated.

### 2.2. Requirements for *Flight Dynamics*

The Aerodynamics sub-module includes functions for aerodynamic forces and moments needed for equations of motion, using only geometric information. Influences of the components of the airplane, for example wing, fuselage, empennage, control surfaces, landing gear and nacelles, need to be considered. Similarly, the correlations between the aerodynamic coefficients, state parameters and deflection of control surfaces have to be taken into account. To simplify the initial modeling process the approach is limited to the correlations shown in Table 1. Furthermore, the models will be reduced to subsonic speeds and will use a simple stall behavior. As seen in Table 1, the influences of control surfaces ailerons, elevator, rudder, horizontal stabilizer and flaps will be respected.

The Equations of Motion will be a system of equations, where all forces and moments are summed up, to get the instantaneous translational and rotational acceleration. With these accelerations the sub-module State Update will calculate the state parameters for the next calculation process. Therefore, integrations and transformations of several coordinate systems are necessary. In some cases of transforming angular velocities singularities may occur. To avoid this, transformations with Quaternions will be used.

Although Landing Gear and Engines belong to Aircraft Systems, they produce forces and moments influencing flight and ground dynamics. The Engines thrust will be modeled with influences of thrust lever position, air speed and altitude. For practical use of Landing Gear a three-point spring damper model is required to map asymmetric landing. Beneath spring damper forces also brakes and friction will be simulated.

## 3. MODELING OF FORCES AND MOMENTS

To simulate flight dynamics, models have to be found that allow calculation of forces and moments affecting the aircraft. This includes models of Aerodynamics, Engines and Landing Gear. This section shows how they are modeled.

### 3.1. Engines

Aircraft engines produce thrust forces and moments depending on distance to CG. Additionally the rotation of blades enforces gyroscopic moments. For this simulation only thrust and its moment will be considered, while

gyroscopic effects will be neglected. To maintain the generic character of the simulation a solution by Thorbeck [2] is used to generate an engine performance map. The equation for the ratio of actual and maximum usable thrust at sea level ( $F^T/F_0^T$ ) is shown in Eq. (1) and is influenced by the throttle valve position  $D$  (between 0 and 1), air speed  $V$ , the atmospheric parameters density  $\rho$ , ambient pressure  $p$  and sonic speed  $a$ . The parameters are necessary at sea level (subscript 0) and flight altitude (without subscript). With an additional constant effectiveness factor  $\eta_T$ , depending on bypass ratio, it is possible to calculate the actual thrust at any altitude or speed. The resulting moment depends on lever arm to CG and incidence angle of nacelles.

$$\frac{F^T}{F_0^T} = \eta_T D \left( \frac{\rho}{\rho_0} \right) e^{-0.35 Ma \left( \frac{p}{p_0} \right) \sqrt{\mu}} \quad (1)$$

### 3.2. Landing Gear

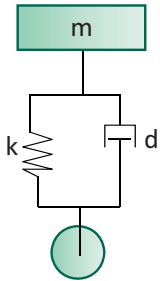


Figure 2: Principle layout of landing gear

One leg of landing gears can be modeled as system of parallel spring and damper (see Figure 2). The produced force depends on the compression ( $l-l_0$ ) of the spring and the compression speed ( $dl/dt$ ). In Eq. (2) the force is calculated with a spring stiffness  $k$  and a viscous damping constant  $d$ . These constants are characteristic parameters for a spring damper and have to be dimensioned. The required spring stiffness is defined by a ratio of maximum

spring force to maximum length deviation (see Eq. (3)). Using a second order differential equation the viscous damping constant can be calculated by setting a desired damping coefficient  $\zeta$  at Eq. (4). The damping coefficient of a stable oscillating system is between 0 and 1 and is chosen depending on the desired behavior of the system. These computations are made for all three legs, representing main landing gears and nose gear. Each leg produces a force predictable with Eq. (2), while compression and its time derivative depend on aircraft attitude and height above ground.

$$F^{SD} = -[k \cdot (l - l_0) + d \cdot \dot{l}] \quad (2)$$

$$k = [m_{\max} (g + \ddot{z}_{\max})] / \Delta l_{\max} \quad (3)$$

$$d = 2\zeta \sqrt{k \cdot m_{\max}} \quad (4)$$

The forces of the spring damper are parallel to the yaw axis of the aircraft. In addition, landing gear produces forces parallel to roll and pitch axis due to friction and brakes. Friction force depends on the normal force to the ground, that is calculated by using the spring damper force (see Eq. (5)), and a friction coefficient. In longitudinal

direction the friction coefficient is smaller than in lateral direction, due to rolling  $\mu_r$  and gliding  $\mu_g$  of the wires (see Eq. (6)). Braking forces can be seen as additional force against the longitudinal direction of the aircraft depending on a braking coefficient  $b$ , which accompanies with the deflection of the brakes. All forces are computed for each leg and are summed up to one force vector. For resulting moments every force is multiplied with its lever arm and summed up to a main moment vector.

$$F_z^{LG} = F^{SD} / (\cos \Phi \cdot \cos \Theta) \quad (5)$$

$$F_x^{LG} = \mu_r F_z^{LG} + b F_{B_{\max}}, \quad F_y^{LG} = \mu_g F_z^{LG} \quad (6)$$

### 3.3. Aerodynamics

The most demanding part of a flight dynamics simulation is to create models for aerodynamics. Certified commercial flight simulators mostly depend on data measured in different states of flight. During simulation linear relations between state variables and forces and moments via aerodynamic coefficients and derivatives can be used. If it is assumed that measured data are not available, information has to be derived using the aircraft geometry only.

The aerodynamic coefficients can be split into the forces drag, side force and lift and moments for rolling, pitching and yawing. Each is modeled with respect to different influences of flight conditions and aircraft components.

#### 3.3.1. Lift

The lift coefficient is mainly influenced by the components wing, horizontal stabilizer and fuselage. Due to interferences between wing and fuselage, it is assumed that the lift due to fuselage is equal to the lift reduction of the wing [3]. Thus, just wing and horizontal stabilizer have to be considered.

The lift of the wing can be split into lift due to basic wing geometry and the lift due to slats and flaps extension. Modeling flaps is described at subsection 3.3.7 while influences of slats will be neglected.

To get the basic lift the lifting-line theory using the method of Multhopp [4] is used. This method splits the wing into small sections and calculates influences between each other. The distribution of lift over the wing can be calculated directly. Additionally information about the airfoil behavior is necessary. This includes two-dimensional lift of the airfoil due to angle of attack. An approach of Schlichting and Truckenbrodt [5] is used and modified for computation, where the airfoil is divided into a convex skeleton and a symmetric drop shape. These shapes are split into panels and each of them gets an infinitesimal circulation. The influences between the single panels cause a velocity distribution, which is synonymous for lift. In addition to lift of airfoils drag due to pressure and pitching moment can be calculated, which is used in subsection 3.3.2 and 3.3.5.

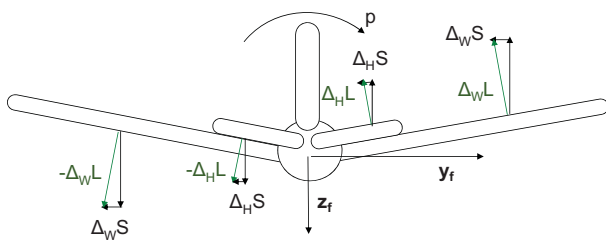


Figure 3: Influence of dihedral to side force

The lift of the stabilizer can be subdivided into a basic lift and lift due to elevator deflection. Modeling the elevator is described in section 3.3.7. The basic lift could also be calculated with the Multhopp-method, but this is not sufficient for wings with small aspect ratio. Thus the method of Weißinger in combination with a correction factor of Roskam [6] is used. This is a dimensioning method with respect to aspect ratio, sweep angle, Mach number and influence of the fuselage. Additional lift is produced when the aircraft pitches. The pitch rate induces an additional angle of attack that influences the known equations just with a single term.

### 3.3.2. Drag

Every component of an aircraft produces drag. Therefore all components are classified into two types, *wing* or *tube*. *Wing* includes main wing, horizontal and vertical stabilizer. Each *wing* produces zero-lift drag and drag due to lift. Zero-lift drag is further partitioned into drag due to pressure and friction. Drag due to pressure of the main wing is already known by the Multhopp method. For the stabilizers a solution of Torenbeek [7] is used, which is a function of the ratio thickness to length. The calculation of drag due to friction is based on assumptions of Blasius and Prantl [8], where friction coefficient is a function of Reynolds number, chord of the *wing* and type of flow (laminar or turbulent). Drag due to lift is calculated with the parabolic function of Lilienthal with respect to the aspect ratio [5].

*Tube* is the generic name for the aircraft components fuselage and engine nacelles. They also produce zero-lift drag and drag due to lift. Here, zero-lift drag is calculated by a second solution of Torenbeek, where drag due to friction and drag due to pressure are combined into one function, depending on ratio diameter to length of the *tube* [7]. The induced drag is approximated with a third order function of angle of attack [7]. The drag coefficient of the landing gear is set as a constant that depends on front area of the gears.

### 3.3.3. Side Force

The aerodynamic side force is mainly influenced by the vertical stabilizer and, in addition, by wing-fuselage combination and horizontal stabilizer. The side force induced by the vertical stabilizer is equivalent to the horizontal stabilizer producing lift force. The same

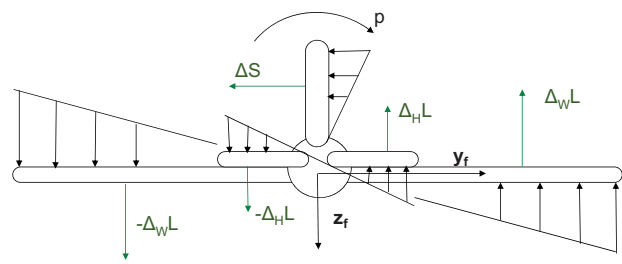


Figure 4: Influence of roll rate to lift and side forces

relationship is used regarding the geometry of the vertical stabilizer with respect to sideslip angle. The influence of the wing-fuselage combination to the sideslip is mapped by an efficiency factor defined by Roskam [6], depending on diameter of the fuselage, area of the horizontal stabilizer, sweep angle, aspect ratio and position of the wing. The influence of yaw rate has the same effect like pitch rate to the horizontal stabilizer. Furthermore, roll rate causes a side force by inducing an additional angle of sideslip component at the vertical stabilizer. The side force also depends on the rudder deflection, described in subsection 3.3.7.

The influence of wing and horizontal stabilizer can be divided into rotation of zero-lift-drag along the flight direction and influences due to dihedral angle. When the aircraft flies asymmetric or rolls, parts of angle of attack and with this additional lift forces are induced. These are orthogonal to the wing surfaces. In case of dihedral angle, portions of side force are generated by these additional lift forces (Figure 3). Note that, the influences of yaw rate and deflection of ailerons are negligible.

### 3.3.4. Rolling Moment

The rolling moment coefficient is mainly influenced by lift and side forces of wing, empennage and their control surfaces. In case of vertical stabilizer, rolling moment is calculated by the product of side force and lever arm to CG. Regarding wing and horizontal stabilizer just asymmetric flight, roll rate or yaw rate cause a rolling moment. Rolling and yawing cause additional angles of attack, that are shown in Figure 4 for roll rate. The resulting local changes in lift and side forces cause moments around the roll axis, with the lever arm to CG.

During asymmetric flight the influence of sweep angle increases. At the windward side the wind flow is more effective than on the leeward side (positive sweep). This is described by angular functions of the sweep angle and angle of sideslip. The side forces affected by dihedral angle (see subsection 3.3.3) cause an additional rolling moment with the respective lever arm to CG. The influence of the fuselage at asymmetric flight can be seen as additional dihedral angle, like it is assumed in [3].



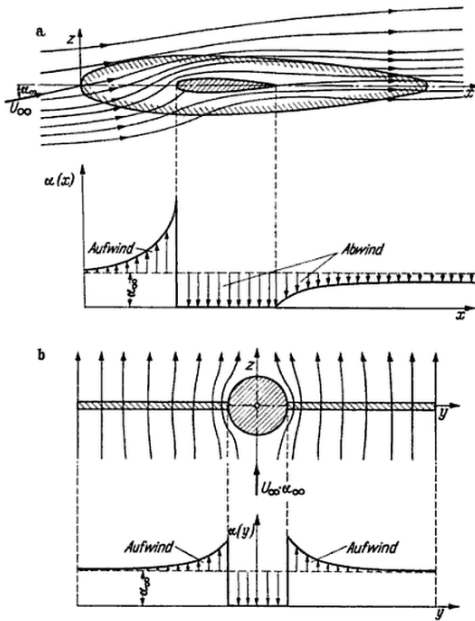


Figure 5: Influence of the wing to angle of attack along the fuselage [3]

### 3.3.5. Pitching Moment

The aircraft components causing pitching moment can be reduced to wing, horizontal stabilizer and fuselage. The lift force by wing, horizontal stabilizer and their control surfaces (elevator, aileron and trailing edge flap) induce one part of the pitching moment together with their lever arms to CG. Additionally the wing produces zero-lift moment, calculated by the Multhopp method.

Further, pitching moment is affected by the flow around the fuselage. Pressure differences produce local lift forces that do not affect the total lift force, but the moment around the pitch axis. This can be described using an expression by Schlichting and Truckenbrodt [3], where the resulting moment coefficient depends on the distribution of angle of attack along the fuselage, the ratio of length and diameter of the tube and the local diameter. This distribution is interfered by the wing (see Figure 5) and is calculated as function of either sweep angle or aspect ratio [3]. For the present simulation both models are combined, such that both influences are considered.

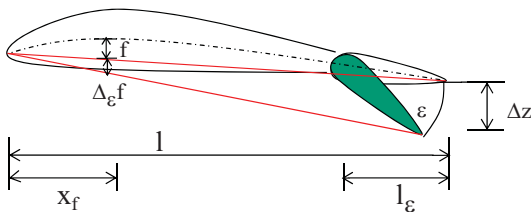


Figure 7: Geometry of a plain flap

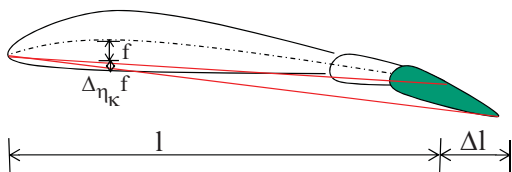


Figure 8: Geometry of a fowler flap

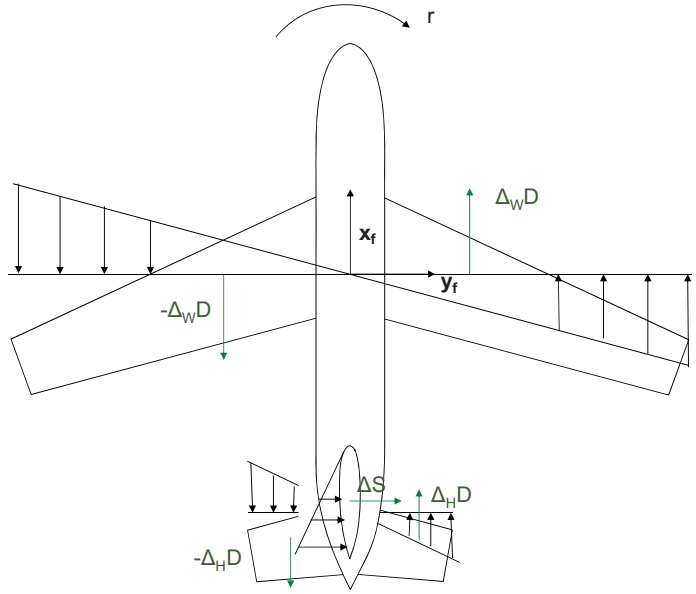


Figure 6: Influence of yaw rate to drag and side forces

### 3.3.6. Yawing Moment

The main portion of the yawing moment is generated by the vertical stabilizer with side force times lever arm to CG. An additional moment is produced with the rising camber by deflection of the rudder (see subsection 3.3.7).

In case of asymmetric flight, rolling or yawing additional lift forces are produced at wing and horizontal stabilizer (see subsection 3.3.3 and 3.3.4). These cause local differences in drag that have no influence to the total drag, but the moment around the yaw axis, like it is shown in Figure 6 for yaw rate. Therefore the yawing moment coefficient of wing and horizontal stabilizer is assumed to be the product of the additional drag coefficient, which can be calculated by the parabolic solution (see subsection 3.3.2), and the lever arm to CG.

The influence of fuselage to yawing moment is similar to pitching moment. The flow around the fuselage causes local side forces, which produce further yawing moment. This can also be expressed with the assumption of Schlichting and Truckenbrodt [3] while the sideslip angle can be assumed to be constant along the fuselage.

### 3.3.7. Control Surfaces

The control surfaces produce additional lift or side forces. For the present simulation model two types of control surfaces are considered: Plain flaps, that just change the camber  $f$  of the airfoil (see Figure 7), and fowler flaps, that change the chord  $l$  of the airfoil (see Figure 8). The plain flaps, like ailerons, elevator and rudder, are modeled with the assumption of the airfoil theory, which says that the angle of attack at zero-lift  $\alpha_0$  is directly equivalent to the camber  $f$  of an airfoil [3]. So it is possible to get the change in angle of attack at zero lift  $\Delta\alpha_0$  by using a geometric function (see Eq. (7)).

$$\Delta\alpha_0 = -2 \frac{\Delta_\epsilon f}{l} = -2 \frac{\Delta z}{l^2} x_f = -2 \frac{l_\epsilon}{l^2} x_f \sin \epsilon \quad (7)$$

With this change of angle of attack (or sideslip in case of rudder) the lift at the control surface changes and also an additional zero-lift moment appears.

In case of fowler flaps the chord of the airfoil changes, which has to be regarded in the chord length  $l$  in the geometric function (7). Also at the calculation of the aerodynamic coefficients a correction factor  $(1+\Delta l/l)$  has to be included because the reference value changes with the chord of the airfoil. Both, fowler and plain flaps are assumed to have a constant position of maximum camber  $x_f$ .

#### 4. IMPLEMENTATION

The mathematic models described in section 3 are implemented as C-code and embedded into Matlab-Simulink®. Matlab-Simulink® is responsible for dispatching the in and out-puts between the modules. Therefore, the simulation architecture described in section 2.1 is used to arrange the models Engines, Landing Gear and Aerodynamics (see Figure 9). In addition, user interfaces were implemented to control and use the simulation. Input can be done by using side stick and thrust lever devices. Output is directed by an existing Matlab-Simulink® interface to the open source flight

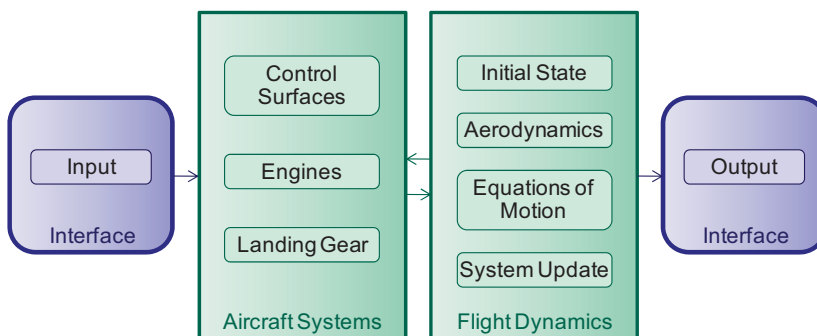


Figure 9: Structure of implemented simulation modules

simulation FlightGear. Information about state parameters, deflections of control surfaces and more can be represented with the visual system of FlightGear. The inputs of the devices are translated into deflections of control surfaces, which is part of Aircraft Systems like Engines and Landing Gear. With these input data and the current state variables, forces and moments of Engines, Landing Gear and Aerodynamics are calculated with the given models. Afterwards they are transformed into the same coordinate system to solve the Equations of Motion. The solutions of the equations are current translational and rotational accelerations. These have to be integrated to get the new state of the system (System Update). The integration is done using existing toolboxes of Matlab-Simulink®. To prevent singularities in transforming angular velocities between different coordinate systems, Quaternions are used in this module like in [9]. With the updated state variables the new iteration can be computed. For the first iteration of calculation, initial states are necessary, that is the reason why an additional block is implemented.

The information about aircraft geometry is mostly necessary for the calculation of Aerodynamics. The

geometric data can be obtained from a scaled three-side view of the airplane. This includes for example the span of the wing, length of the fuselage, distribution of wing chord and positions of the root of vertical and horizontal stabilizer. With these essential data secondary information is calculated, for example wing area, neutral point of wing and empennage, and wetted area of the fuselage.

The resulting system allows simulation of the behavior of an aircraft with the knowledge of geometry. On the one hand, it is possible to fly the aircraft directly with the input devices and to observe the response in an outside view provided by FlightGear. On the other hand, it is also usable to examine the behavior of the aircraft by using given input variables over time.

#### 5. FLIGHT TESTS AND PRELIMINARY VALIDATION OF THE GENERIC FLIGHT SIMULATION

To validate the generic flight simulation, some reference data were necessary. Therefore a level DG [10] certified FFS by CAE, simulating an Airbus A330, was used. It was possible to record the simulation variables at different states of flight. State variables, control surface deflections, force coefficients and moment coefficients were recorded for validation. Reference data were generated for trimmed flights at different speeds, horizontal and climbing flights at steady state and unsteady maneuver flights.

The present generic simulation, called  $\diamond\text{Sim}^1$ , was validated from two points of view. The first is the validation of the static coefficients and the second is the dynamic behavior.

##### 5.1. Static Validation

For static validation, aerodynamic force and moment coefficients were compared to those of the certified simulation, called CAE-Sim in this paper. Therefore, flights at different speeds and flaps setting (Airbus convention) were performed at flight altitude of 5000ft and with an aircraft mass of 168 tons. At Table 2 an overview about the test points for static validation is given. For these points the same configuration, control surface deflections and state variables were used to calculate the aerodynamic coefficients with  $\diamond\text{Sim}$ . To compare the measured and calculated coefficients, the absolute and relative error was calculated (see Eq. (8) and (9)). The results of configuration 1 and 3 are shown in Figure 10 and Figure 11.

Configuration	Flaps Setting	State n speeds [kt]
1	0	250, 200, 190, 180, 170, 160
2	2	180, 160, 140, 130, 120
3	3	180, 160, 140, 120
4	4	180, 170, 160, 150, 120, 110

Table 2: Configurations for static validation

<sup>1</sup> pronounced Karo-Sim

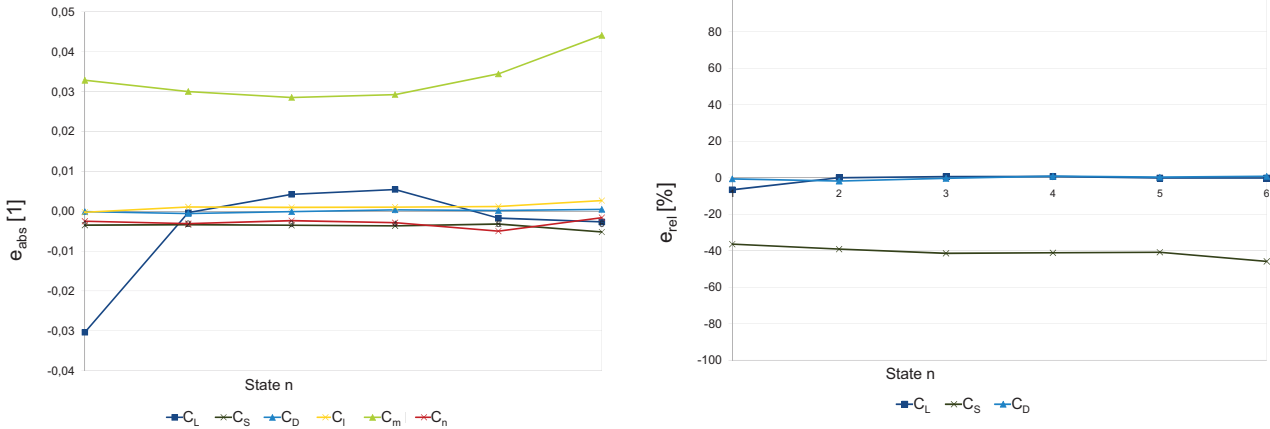


Figure 10: Absolute and relative error of aerodynamic coefficients at different states, configuration 1

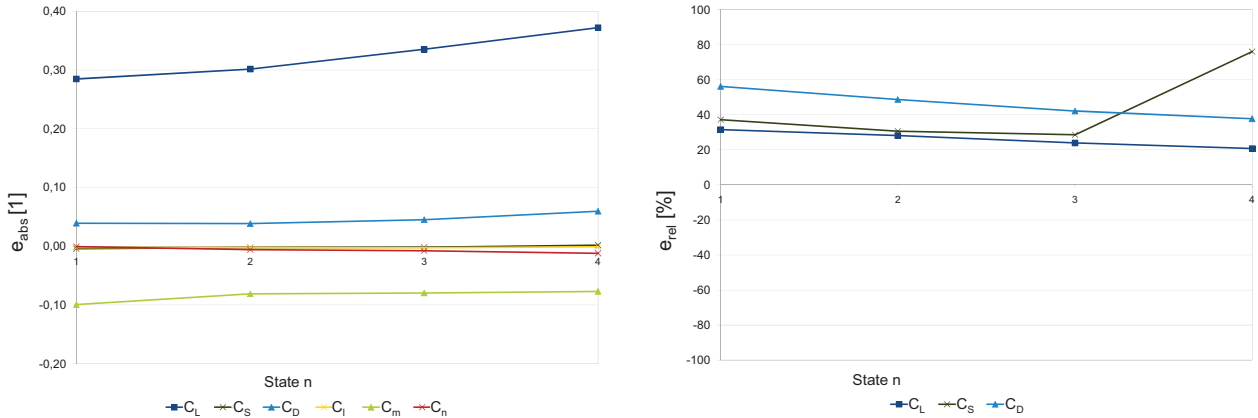


Figure 11: Absolute and relative error of aerodynamic coefficients at different states, configuration 3

$$e_{abs} = x_{measured} - x_{calc} \quad (8)$$

$$e_{rel} = e_{abs} / |x_{measured}| \quad (9)$$

Figure 10 shows, that the absolute errors of coefficients for lift and drag are depending on speed, but the relative errors are nearly constant under 2%. The relative error of side force coefficient depends on speed, but the absolute error is at a constant deviation. This indicates, that a constant value can correct the calculation. For coefficients of yawing and rolling moments it can be seen, that the absolute deviations are small. In case of pitching moment the absolute error is more pregnant.

Figure 11 shows the errors of configuration 3, where flaps are extended. For lift and drag coefficient it can be seen, that the relative errors are nearly constant, but the coefficients of  $\diamond$ Sim are lower. This shows that the model for flaps is not precise enough for simulation. Note that the extension of slats is not modeled by  $\diamond$ Sim, but in CAE-Sim. This is one reason, why deviations appear between both simulations. The behavior of the yawing and rolling moment at the absolute error has not changed much to configuration 1 and the error of pitching moment is also too high in value.

Some reasons of the high errors in moment coefficients are uncertainties about the calculation process of the CAE-Sim, not respected aircraft components, like slats or roll spoiler, and possible wrong geometry information. Every small failure in modeling has effects to the forces

and moments, which leads to not reaching the trimmed state at the same states of flight and control surface deflections.

## 5.2. Dynamic Validation

The second part of validation is to compare the dynamic behavior of  $\diamond$ Sim with the CAE-Sim. Therefore horizontal and climbing flights at steady state and unsteady flights, with trimmed conditions at initial state and aircraft mass of 168 tons, were performed (see Table 3).

#	Time [s]	Altitude [m]	Speed [m/s]	Characteristic
1	7.3	1570	170	Horizontal, steady state
2	7.3	4590	200	Horizontal, steady state
3	7.3	2830	230	Climb, steady state
4	150	2860	270	Descend maneuver, unsteady

Table 3: Test flights for dynamic validation

The recorded initial states and control surface deflections should be used as input for  $\diamond$ Sim. As seen at the static validation, trimmed flight could not be reached with the input data of CAE-Sim. That is why  $\diamond$ Sim was initially trimmed for each reference speed. To these necessary control surface deflections  $\varepsilon_{\diamond Sim}(0)$  the deviation to the initial deflections of CAE-Sim ( $\varepsilon_{CAE-Sim}(t) - \varepsilon_{CAE-Sim}(0)$ ) were added

(see Eq. (10)). These synthetic deflections  $\varepsilon_{\diamond Sim}(t)$  were finally used as input for  $\diamond Sim$  to validate the dynamic behavior. Thus, an equal basis was created to compare both simulations.

$$\varepsilon_{\diamond Sim}(t) = \varepsilon_{\diamond Sim}(0) + (\varepsilon_{CAE-Sim}(t) - \varepsilon_{CAE-Sim}(0)) \quad (10)$$

Figure 12 shows the results of altitude and air speed for test flight 2. After 7 seconds the error is less than 2m respectively 0.5m/s. This shows that a horizontal flight, initialized to a trimmed state and with the same deviation of control surface deflection of CAE-Sim, is possible in the same way like the reference model.

Figure 13 shows the comparison of the dynamic behavior for an unsteady flight after an 3-2-1-1 elevator input. After 150s the deviation in altitude is approximately 15m, but the dynamic of the phugoid mode is not as pronounced as with the reference model. The speed error after 150s is less than 2m/s, but also the maximum amplitude is not reached. This shows that the energy states of both simulations are nearly the same, but the effectiveness of the control surface is too low. That result enforces the conclusion of the static validation that the models for the control surfaces have to be improved for better simulation.

The inadequate model of control surface is also one reason for the behavior of the simulated aircraft at its lateral movement, shown in form of the bank angle. While the CAE-Sim captures a constant bank angle after 20s,  $\diamond Sim$  rolls further with a nearly constant rotation rate. This also influences the yaw angle, which is not shown here. The ailerons of CAE-Sim are deflected opposed but with different values. Hence, the local lift forces at both sides of the wing of  $\diamond Sim$  differ to those of the reference models. This leads to a non-zero rolling moment and causes the shown rolling movement. Furthermore the simulated aircraft uses roll spoiler at flight, which is not modeled at  $\diamond Sim$  and causes additional rolling moments.

## 6. CONCLUSIONS

A flight simulation using solely the geometric data of an aircraft to reproduce its dynamic behavior is presented. With the generic and modular characteristics, a basis was laid for a simulation approach that can be adapted of different kinds of aircraft.

The structure of the complete flight simulation was defined in order to separate different functions into different modules. For these modules, requirements and interfaces to other modules were set.

The main part of this work referred to modeling of aircraft dynamics, including models for aerodynamics, engine thrust and landing gear. The development of these models relied on different methods, e.g. existing design methods, modified assumptions of aerodynamicists, and flight mechanical dependencies.

With the environment of Matlab-Simulink®, embedded C-code and FlightGear, the simulation framework was implemented and preliminary validated according to data of a certified FFS. The results of the validation confirm that

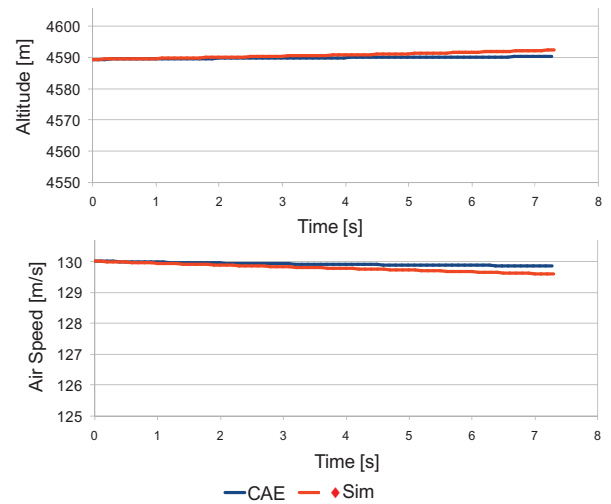


Figure 12: Comparison of altitude and speed for test flight 2, horizontal flight at steady state

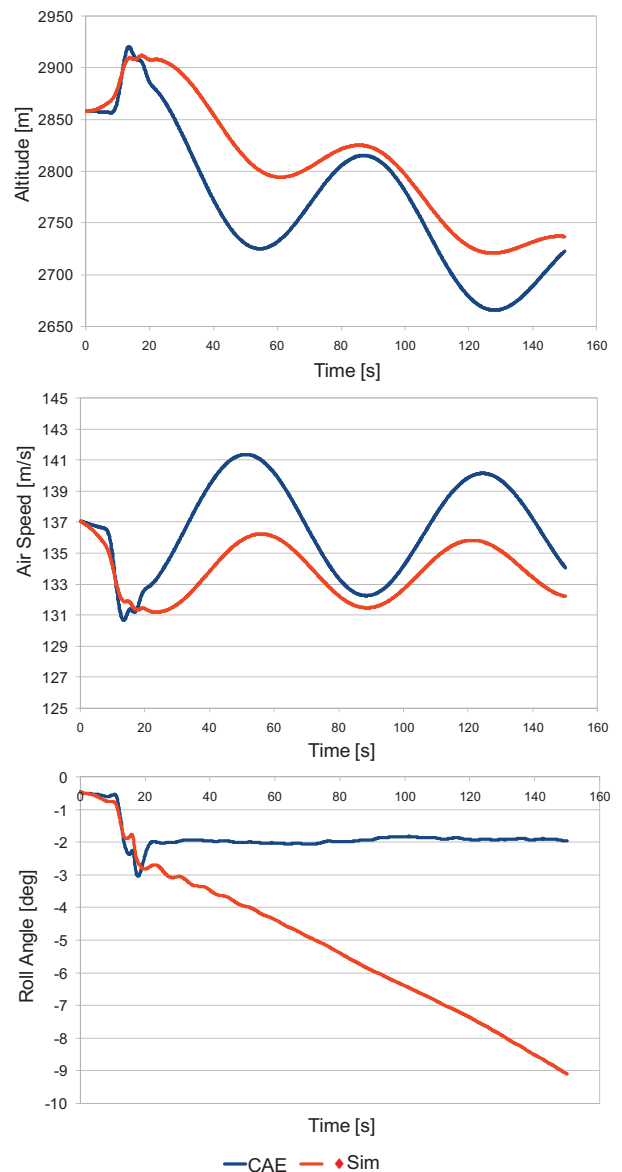


Figure 13: Comparison of altitude, air speed and bank angle for test flight 4, transient descending flight



the initial version of ◇Sim works properly. However there have to be further improvements in aerodynamic modeling.

## References

- [1] Schreiter, K.: *Entwicklung und Validierung eines generischen Flugsimulationsmodells auf Basis von Flugzeuggeometriedaten für zukünftige Forschungsvorhaben im Bereich Flugführung und Flugregelung*. Diplomarbeit, Department of Aeronautics and Astronautics, TU Berlin, Berlin 2010
- [2] Thorbeck, J.: *Ein Beitrag zum rechnergestützten Entwurf von Verkehrsflugzeugen*. Ph.D. Dissertation, Department of Aeronautics and Astronautics, TU Berlin, Berlin 1984
- [3] Schlichting, H. ; Truckenbrodt, E. A.: *Aerodynamik des Flugzeuges, Band 2: Aerodynamik des Tragflügels (Teil II), des Rumpfes, der Flügel-Rumpf-Anordnung und der Leitwerke*. Springer-Verlag Berlin Heidelberg, 1959, 2001
- [4] Multhopp, H.: *Methods for Calculating the Lift Distribution of Wings (Subsonic Lifting-Surface Theory)*. R. & M. No. 2884, Brit. A.R.C., Jan. 1950.
- [5] Schlichting, H. ; Truckenbrodt, E. A.: *Aerodynamik des Flugzeuges, Band 1: Grundlagen der Strömungstechnik, Aerodynamik des Tragflügels (Teil I)*. Springer-Verlag Berlin Heidelberg, 2001
- [6] Roskam, J.: *Airplane Design, Part VI: Preliminary Calculation of Aerodynamic, Thrust and Power Characteristics*. Roskam Aviation and Engineering Corporation, 1987
- [7] Torenbeek, E.: *Synthesis of Subsonic Airplane Design*. Kluwer Academic Publisher, Delft University Press, 1982
- [8] Anderson, J. D.: *Fundamentals of Aerodynamics*. 2<sup>nd</sup> edition, McGraw-Hill, Inc., 1991
- [9] Allerton, D.; Moir, I.; Seabridge, A.; Langton, R.: *Principles of Flight Simulation*. John Wiley & Sons Ltd., Chichester (GB), 2009
- [10] - : JAR 1A.030 Aeroplane Flight Simulators. Joint Aviation Authorities July 2003